

WindowNet: Learnable Windows for Chest X-ray Classification

Alessandro Wollek^a, Sardi Hyska^b, Bastian Sabel^b, Michael Ingrischi^b,
Tobias Lasser^a

^a*Munich Institute of Biomedical Engineering, and School of Computation, Information,
and Technology, Technical University of Munich, Boltzmannstr.*

11, Garching, 85748, Bavaria, Germany

^b*Department of Radiology, University Hospital*

Ludwig-Maximilians-University, Marchioninistr. 15, Munich, 81337, Bavaria, Germany

Abstract

Public chest X-ray (CXR) data sets are commonly compressed to a lower bit-depth to reduce their size, potentially hiding subtle diagnostic features. In contrast, radiologists apply a windowing operation to the uncompressed image to enhance such subtle features. While it was shown that windowing improves classification performance on computed tomography (CT) images, the impact of such an operation on CXR classification performance remains unclear. In this study, we show that windowing strongly improves CXR classification performance of machine learning models, and propose WindowNet, a model that learns multiple optimal window settings. Our model achieved an average AUC score of 0.812 compared to 0.759 by a commonly used architecture without windowing capabilities on the MIMIC data set. Our code is publicly available at <https://gitlab.lrz.de/IP/windownet>.

Keywords: windowing, chest X-ray, chest radiograph, bit-depth, classification, deep learning

1. Introduction

To better differentiate subtle pathologies, chest X-rays (CXR) are commonly acquired with a high bit-depth. For example, the images in the MIMIC data set provide 12-bit gray values, see Johnson et al. (2019). However, to reduce the file size and save bandwidth, these images are often compressed

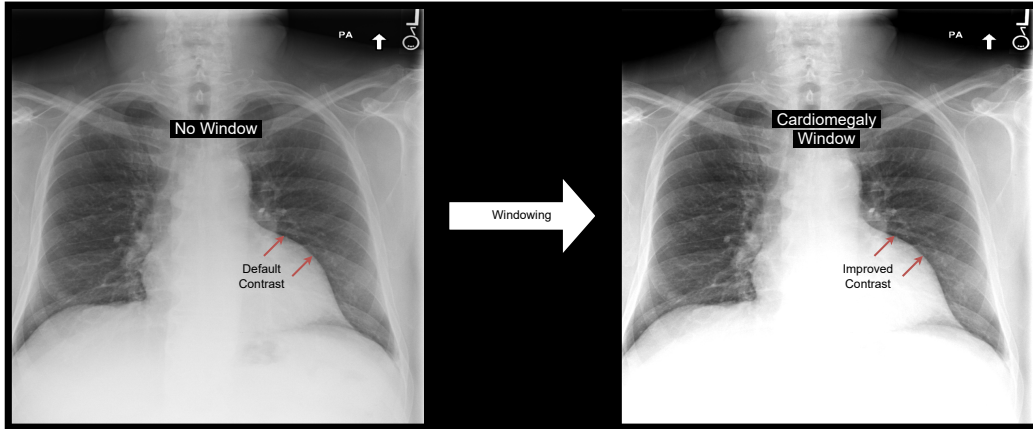


Figure 1: Applying a windowing operation enhances the contrast of particular structures of an image. For example, the depicted windowing operation improved cardiomegaly classification performance on the MIMIC data set.

to a lower bit-depth. The Chest X-ray 14 data set, for example, was reduced to 8-bit depth before publication (Wang et al., 2017).

Under optimal conditions, the human eye can differentiate between 700 and 900 shades of gray, or 9- to 10-bit depth (Kimpe and Tuytschaever, 2007). Hence, radiologists cannot differentiate all 12-bit gray values when inspecting a chest X-ray. To better identify subtle contrasts, they apply a windowing operation to the image: they increase the contrast by limiting the range of gray tones (see Figure 1). These windowing operations can be specified by their center (level) and width.

In contrast to chest radiographs, gray values in computed tomography (CT) images are calibrated to represent a specific Hounsfield unit (HU) (Maier et al., 2018). For example, a HU value of -1000 corresponds to air, 0 HU to distilled water at standard pressure and temperature, bones range from 400 HU to 3000 HU (Maier et al., 2018). To highlight the lung in a chest CT image, one could apply a window with a level of -600 HU and width of 1500 HU (Kazerooni and Gross, 2004). In other words, everything below -1350 HU is displayed as black and above 150 HU as white. Consequently, more distinct gray tone values can be used for the specified range, resulting in a higher contrast.

For CT images, several studies showed that windowing improves classification performance of deep neural networks (Karki et al., 2020; Huo et al., 2019; Lee et al., 2018; Kwon and Choi, 2020). For CXR, no quantitative scale

like the Hounsfield Unit exists. Nevertheless, radiologists window CXR for enhanced contrasts during inspection. Furthermore, depending on the region of interest, they use different window settings. This observation leads to the following research questions: does windowing affect chest X-ray classification performance and if yes, can windowing improve it? To the best of our knowledge, so far, chest X-rays are commonly processed by a deep learning model without applying any windowing operation (for example, (Rajpurkar et al., 2017; Wollek et al., 2023a)). This study investigates the effect of windowing on chest X-ray classification and proposes a model, WindowNet, that learns optimal windowing settings.

Our contributions are:

- We show that a higher bit-depth (8-bit vs. 12-bit) improves chest X-ray classification performance.
- We demonstrate that applying a window to the chest radiograph as a pre-processing step increases classification performance.
- We propose WindowNet, a chest X-ray classification model that learns optimal windowing settings.

2. Materials and Methods

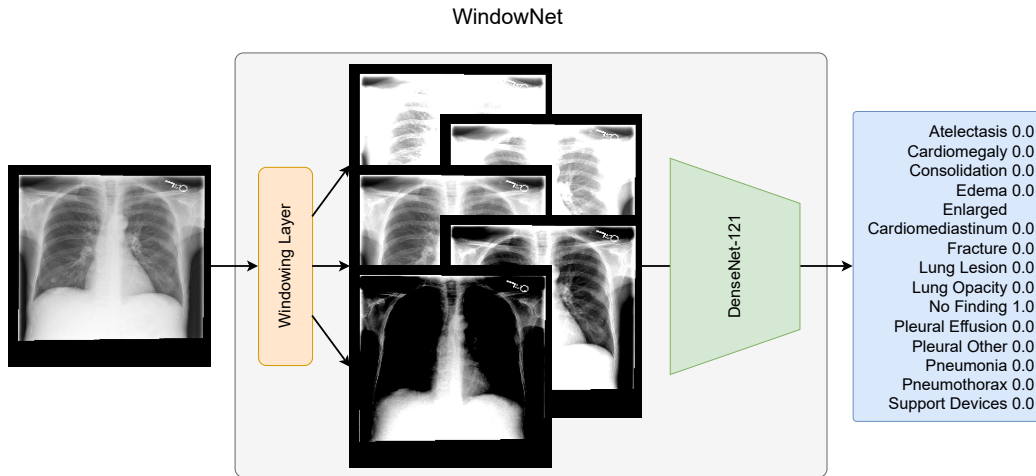


Figure 2: Optimal multi-window chest X-ray classification. Our proposed WindowNet architecture learns to optimize multiple windows for improved classification.

2.1. Data Set

To investigate the importance of windowing on chest X-ray classification we selected the MIMIC data set, as it is the only publicly available, large-scale chest X-ray data set with full bit-depth (Johnson et al., 2019). The MIMIC data set provides chest radiographs in the original Digital Imaging and Communications in Medicine (DICOM) format with 12-bit depth gray values, containing 377,110 frontal and lateral images from 65,379 patients. The images have been labeled according to the 14 CheXpert classes: atelectasis, cardiomegaly, consolidation, edema, enlarged cardiomeastinum, fracture, lung lesion, lung opacity, no finding, pleural effusion, pleural other, pneumonia, pneumothorax, and support devices (Irvin et al., 2019). In our experiments, we used the provided training, validation, and test splits. During pre-processing, the images were resized to 224×224 pixels.

2.2. Architectures

2.2.1. Baseline

As a baseline model (Baseline) for all experiments, we used a DenseNet-121 (Huang et al., 2017) pre-trained on ImageNet (Deng et al., 2009) that is commonly used for chest X-ray classification (Rajpurkar et al., 2017; Wollek et al., 2023b; Xiao et al., 2023). For fine-tuning, we replaced the classification layer with a 14-dimensional fully-connected layer.

2.2.2. WindowNet

To incorporate windowing into the model architecture, we extended the baseline architecture by prepending a windowing layer, as illustrated in Figure 2. In the following, we refer to this model as WindowNet.

We implemented the windowing operation as a 1×1 convolution with clamping, similar to (Lee et al., 2018). This implementation of windowing utilizing convolutional kernels enables the model to learn and use multiple windows in parallel. As the pre-trained DenseNet-121 expects three input channels, we added an additional 1×1 convolution with three output channels after the windowing operation. Following the windowing layer, the images are scaled to the floating point range (0.0, 255.0) and then normalized according to the ImageNet mean and standard deviation.

2.2.3. Training

Both models were trained with binary cross-entropy loss, AdamW optimization with a learning rate of $1e-4$ (Loshchilov and Hutter, 2019), and a

batch size of 32. During training, the learning rate was divided by a factor of 10 if the validation loss did not improve in three consecutive epochs. The training was stopped if the validation loss did not improve after 5 consecutive epochs. The final models were selected based on the checkpoint with the highest mean validation area under the receiver operating characteristic curve (AUC).

2.3. Experiments

2.3.1. 8-Bit vs. 12-Bit

As applying a windowing operation in our experiments required a higher initial bit-depth than conventionally used for chest X-ray image classification, we first tested the effect of bit-depth on classification performance. We trained the baseline model with 8-bit and 12-bit depth and compared mean, and class-wise AUC scores. In both settings no windowing operation was applied. However, the 12-bit images were still scaled to the floating point range (0.0, 255.0). In both settings, the images were normalized according to the ImageNet mean and standard deviation.

2.3.2. Single Fixed Window

To investigate whether windowing has an effect on classification performance, we trained the baseline model with a single fixed windowing operation applied to the 12-bit CXRs. After windowing, the images were scaled to have a maximum value of 255 and normalized according to the ImageNet mean and standard deviation.

For windowing, we use a fixed window level of 100, and levels ranging from 250 to 3500 in steps of 250. All levels were combined with fixed window widths of 500, 1000, 1500, 2000, and 3000. For evaluation, we compared the mean and class-wise AUCs of each model to the baseline with no windowing, i.e., a window level of 2048 and width of 4096.

2.3.3. Trainable Multi-Windowing

To test if end-to-end optimized windows improve chest X-ray classification performance we compared our proposed WindowNet to the baseline and a modified WindowNet without clamping in the windowing layer (No Windowing), i.e., a conventional 1×1 convolutional layer.

In our experiments, we used 14 windows based on the set of class-wise top-3 windows found during the single window experiment and the additional full-range “window”. The selection was based on the validation results. We

initialized the learnable windows with the resulting windows (level, width): (100, 3000), (1250, 1000), (1500, 3000), (1750, 2000), (1750, 3000), (2000, 2000), (2250, 2000), (2250, 3000), (2500, 2000), (2500, 3000), (2750, 3000), (3250, 1000), (750, 3000), and (2048, 4096). The comparison model, “No Windowing”, having a conventional 1×1 convolution, was default initialized using kaiming initialization (He et al., 2015).

3. Theory

A windowing operation can be described by its center (window level) and width (window width). Formally, the windowing operation applied to a pixel value px can be defined as:

$$\begin{aligned} \text{window}(px) &= \min(\max(px, L), U), \\ U &= WL + \frac{WW}{2}, \\ L &= WL - \frac{WW}{2}. \end{aligned}$$

Where U is the upper limit and L the lower limit of the window defined by the window level WL and window width WW .

For efficient training, the windowing operation can be re-written using a clamped 1×1 convolution. Here, the weight matrix is initialized as $W = \frac{U}{WW}$ and the bias term as $b = -\frac{U}{WW}L$, similar to (Lee et al., 2018):

$$\begin{aligned} \min(\max(Wx + b, 0), U) &= \min\left(\max\left(\frac{U}{WW}x - \frac{U}{WW}L, 0\right), U\right) \\ &= \min\left(\max\left(\frac{U}{WW}(x - L), 0\right), U\right) \\ &= \min(\max(x - L, 0), U) \\ &= \min(\max(x, L), U). \end{aligned}$$

Finding	8-Bit	12-Bit
Atelectasis	0.751	0.749
Cardiomegaly	0.770	0.774
Consolidation	0.740	0.742
Edema	0.831	0.833
Enlarged Cardiomedastinum	0.691	0.701
Fracture	0.664	0.710
Lung Lesion	0.680	0.682
Lung Opacity	0.680	0.690
No Finding	0.789	0.797
Pleural Effusion	0.883	0.879
Pleural Other	0.823	0.831
Pneumonia	0.659	0.698
Pneumothorax	0.802	0.828
Support Devices	0.868	0.888
Mean	0.759	0.772

Table 1: Effect of bit-depth on chest X-ray classification performance. A higher bit-depth improved AUC values for most (12/14) classes. Higher values are highlighted in bold.

To recover the window level and width after training, we compute:

$$\begin{aligned}
 WW &= \frac{U}{W}, \\
 WL &= -\frac{b}{W} + \frac{WW}{2}.
 \end{aligned}$$

4. Results

4.1. 8-Bit vs. 12-Bit

The classification AUCs, when trained with 8-bit or 12-bit depth, are shown in Table 1. Training with 12-bit images improved the average classification performance compared to 8-bit images (0.772 vs. 0.759 AUC). Also, most (12/14) class-wise AUCs increased when training with a higher bit-depth. The only exceptions were atelectasis and pleural effusion, where training with 8-bit images resulted in slightly higher AUC with 0.751 vs. 0.749 and 0.883 vs. 0.879, respectively.

Finding	No Window	Best Fixed Window
Atelectasis	0.749 (2048, 4096)	0.757 (2750, 3000)
Cardiomegaly	0.774 (2048, 4096)	0.786 (1750, 3000)
Consolidation	0.742 (2048, 4096)	0.744 (2500, 3000)
Edema	0.833 (2048, 4096)	0.841 (1750, 3000)
Enlarged Cardiom.	0.701 (2048, 4096)	0.734 (2250, 3000)
Fracture	0.710 (2048, 4096)	0.706 (1000, 3000)
Lung Lesion	0.682 (2048, 4096)	0.720 (2500, 3000)
Lung Opacity	0.690 (2048, 4096)	0.690 (2250, 3000)
No Finding	0.797 (2048, 4096)	0.804 (2500, 3000)
Pleural Effusion	0.879 (2048, 4096)	0.888 (2500, 3000)
Pleural Other	0.831 (2048, 4096)	0.850 (2750, 3000)
Pneumonia	0.698 (2048, 4096)	0.690 (1750, 3000)
Pneumothorax	0.828 (2048, 4096)	0.832 (1750, 3000)
Support Devices	0.888 (2048, 4096)	0.889 (2750, 3000)
Mean	0.772 (2048, 4096)	0.775 (2500, 3000)

Table 2: Effect of fixed windowing on chest X-ray classification AUCs. For each finding, the best performing window and the baseline without no windowing are reported. Higher AUCs values are highlighted in bold. Enlarged Cardiom. = enlarged cardiomedastinum.

4.2. Single Fixed Window

The results of training with fixed window chest X-rays are reported in Table 2. They demonstrate that windowing improved chest X-ray classification AUCs for most classes (12/14) except for fracture and pneumonia with AUCs of 0.710 vs. 0.706 and 0.698 vs. 0.690, respectively. On average, the window with level 2500 and width 3000 performed slightly better than the full range with an AUC of 0.775 vs. 0.772. Across all windows, a window width of 3000 performed best with varying window levels.

A comparison of the four best-performing windows to the baseline is shown in Table 3. All five settings achieved similar average AUC scores. No single window performed consistently better across all classes, suggesting that multiple windows could overall improve the classification performance.

4.3. Trainable Multi-Windowing

The effect of learning multiple optimal windows using our proposed WindowNet is reported in Table 4, comparing it to the baseline and the Win-

Window	None (Baseline)	#1	#2	#3	#4
Level	2048	2500	1750	2750	2250
Width	4096	3000	3000	3000	3000
Finding					
Atelectasis	0.749	0.756	0.753	0.749	0.757
Cardiomegaly	0.774	0.783	0.786	0.774	0.777
Consolidation	0.742	0.744	0.743	0.742	0.740
Edema	0.833	0.830	0.841	0.833	0.831
Enlarged Cardiom.	0.701	0.710	0.700	0.701	0.686
Fracture	0.710	0.695	0.670	0.710	0.669
Lung Lesion	0.682	0.720	0.710	0.682	0.700
Lung Opacity	0.690	0.683	0.686	0.690	0.684
No Finding	0.797	0.804	0.800	0.797	0.798
Pleural Effusion	0.879	0.888	0.883	0.879	0.885
Pleural Other	0.831	0.841	0.820	0.831	0.850
Pneumonia	0.698	0.686	0.690	0.698	0.683
Pneumothorax	0.828	0.822	0.832	0.828	0.809
Support Devices	0.888	0.887	0.887	0.888	0.889
Mean (Validation)	0.804	0.807	0.802	0.805	0.803
Mean (Test)	0.772	0.775	0.772	0.772	0.768

Table 3: Best fixed single window settings for chest X-ray classification found during grid search. The class-wise AUCs of the four best performing windows (Window 1-4) and the baseline without windowing are reported. Additionally, mean validation AUCs are provided. Highest AUC values are highlighted in bold. Enlarged Cardiom. = enlarged cardiome-diastinum.

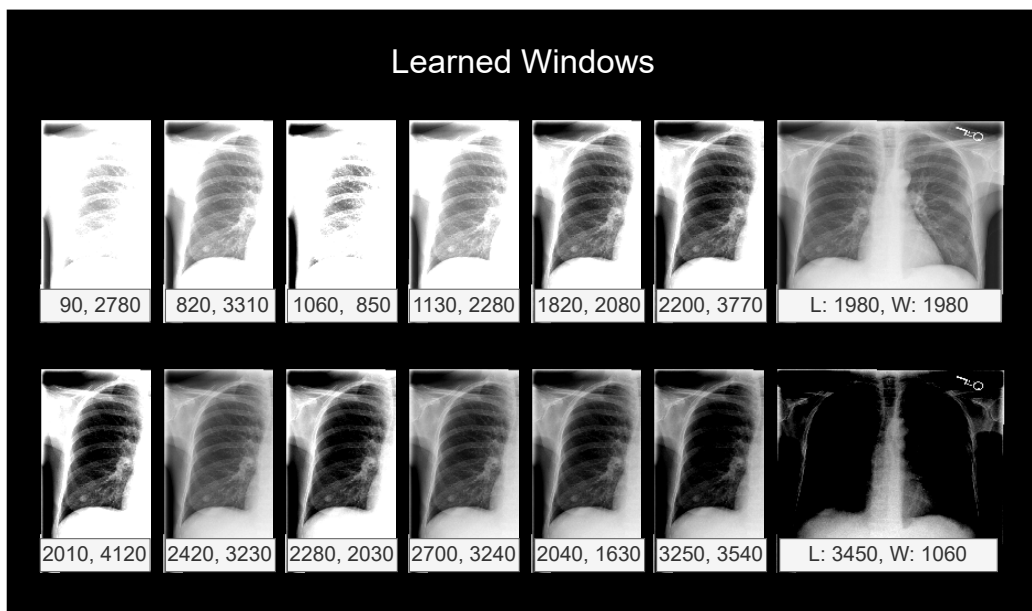


Figure 3: Windows learned during the training of WindowNet. For window initialization the following window levels (L) and widths (W) were used (level, width): (100, 3000), (1250, 1000), (1500, 3000), (1750, 2000), (1750, 3000), (2000, 2000), (2250, 2000), (2250, 3000), (2500, 2000), (2500, 3000), (2750, 3000), (3250, 1000), (750, 3000), and no window (2048, 4096).

Finding	8-Bit	No Windowing (12-Bit)	WindowNet (12-Bit)
Atelectasis	0.751	0.812	0.829
Cardiomegaly	0.770	0.814	0.827
Consolidation	0.740	0.808	0.823
Edema	0.831	0.891	0.897
Enlarged Cardiom.	0.691	0.745	0.764
Fracture	0.664	0.619	0.615
Lung Lesion	0.680	0.701	0.744
Lung Opacity	0.680	0.726	0.745
No Finding	0.789	0.855	0.859
Pleural Effusion	0.883	0.909	0.918
Pleural Other	0.823	0.721	0.793
Pneumonia	0.659	0.731	0.750
Pneumothorax	0.802	0.830	0.886
Support Devices	0.868	0.897	0.918
Mean	0.759	0.790	0.812

Table 4: Comparison of baseline (8-Bit), WindowNet without windowing (“No Windowing 12-Bit”) and WindowNet (12-Bit) AUCs for chest X-ray classification. Higher values are highlighted in bold. Enlarged Cardiom. = enlarged cardiomeastinum.

WindowNet architecture without windowing (“No Windowing”). Overall, WindowNet performed considerably better with an average AUC of 0.812 compared to 0.750 of the 8-bit baseline. When compared to a conventional 1×1 convolution in the WindowNet architecture (“No Windowing”) the results demonstrate the improvement of windowing with an average AUC of 0.812 vs. 0.790.

For nearly all classes (12/14) our proposed WindowNet model achieved a higher AUC. For example, pneumothorax classification AUC improved from 0.802 to 0.886 with windowing. Only for the fracture and pleural other class the baseline model performed better with an AUC of 0.664 vs. 0.615 and 0.823 vs. 0.793, respectively.

The windows learned after training are shown in Figure 3. The model learned a diverse set of windows, with levels from 90 to 3450 and widths from 850 to 4120.

5. Discussion

In this study, we investigated the importance of windowing, inspired by radiologists. Our results show that our proposed multi-windowing model, WindowNet, considerably outperformed a popular baseline architecture with a mean AUC of 0.812 compared to 0.759 (see Table 4). As a necessary pre-condition, we also demonstrated that the common bit-depth reduction negatively affected classification performance (0.759 vs. 0.772 AUC), as seen in Table 1.

Similarly to related work in the CT domain (Lee et al., 2018; Karki et al., 2020; Kwon and Choi, 2020), our results show that windowing is a useful pre-processing step for neural networks operating on chest X-rays. These findings are also in line with the observed manual windowing performed by radiologists in their daily practice. In addition, like radiologists apply multiple windows when inspecting a single image, no single window was better across classes, including not windowing at all (see Table 2).

When comparing our proposed WindowNet with the same architecture but without windowing, in other words, a conventional 1×1 convolution, our results showed that the windowing operation is an important aspect of the architecture (see Table 4). When inspecting the learned windows, see Figure 3, the windows converged to 14 different settings. This provides further evidence that multiple windows are important for classification performance.

While our study’s results are promising, limitations include the exploratory nature of the study and the evaluation on a data set from a single institution, due to lack of other high bit depth public data sets. Further research is needed to show generalization to other data sets and institutions. Another limitation is that the model learns general windowing settings. In contrast, radiologists adapt the windowing setting based on the specific image. Future work could investigate an image-based window setting prediction layer.

In conclusion, we believe our work offers an important contribution to the field of computer vision and radiology by demonstrating that multi-windowing strongly improves chest X-ray classification performance, as shown by our proposed model, WindowNet.

6. Acknowledgments

This work was supported in part by the German federal ministry of health’s program for digital innovations for the improvement of patient-centered care in healthcare [grant agreement no. 2520DAT920].

References

- Deng, J., Dong, W., Socher, R., Li, L.J., Li, K., Fei-Fei, L., 2009. ImageNet: A large-scale hierarchical image database, in: 2009 IEEE Conference on Computer Vision and Pattern Recognition, pp. 248–255. doi:10.1109/CVPR.2009.5206848.
- He, K., Zhang, X., Ren, S., Sun, J., 2015. Delving Deep into Rectifiers: Surpassing Human-Level Performance on ImageNet Classification, in: 2015 IEEE International Conference on Computer Vision (ICCV), IEEE, Santiago, Chile. pp. 1026–1034. doi:10.1109/ICCV.2015.123.
- Huang, G., Liu, Z., Van Der Maaten, L., Weinberger, K.Q., 2017. Densely connected convolutional networks, in: Proceedings of the IEEE Conference on Computer Vision and Pattern Recognition, pp. 4700–4708. arXiv:1608.06993.
- Huo, Y., Tang, Y., Chen, Y., Gao, D., Han, S., Bao, S., De, S., Terry, J.G., Carr, J.J., Abramson, R.G., Landman, B.A., 2019. Stochastic tissue window normalization of deep learning on computed tomography. *Journal of Medical Imaging* 6, 044005. doi:10.1117/1.JMI.6.4.044005.

- Irvin, J., Rajpurkar, P., Ko, M., Yu, Y., Ciurea-Ilcus, S., Chute, C., Marklund, H., Haghighi, B., Ball, R., Shpanskaya, K., 2019. Chexpert: A large chest radiograph dataset with uncertainty labels and expert comparison, in: Proceedings of the AAAI Conference on Artificial Intelligence, pp. 590–597.
- Johnson, A.E., Pollard, T.J., Berkowitz, S.J., Greenbaum, N.R., Lungren, M.P., Deng, C.y., Mark, R.G., Horng, S., 2019. MIMIC-CXR, a de-identified publicly available database of chest radiographs with free-text reports. *Scientific Data* 6.
- Karki, M., Cho, J., Lee, E., Hahm, M.H., Yoon, S.Y., Kim, M., Ahn, J.Y., Son, J., Park, S.H., Kim, K.H., Park, S., 2020. CT window trainable neural network for improving intracranial hemorrhage detection by combining multiple settings. *Artificial Intelligence in Medicine* 106, 101850. doi:10.1016/j.artmed.2020.101850.
- Kazerooni, E.A., Gross, B.H., 2004. *Cardiopulmonary Imaging*. Lippincott Williams & Wilkins.
- Kimpe, T., Tuytschaever, T., 2007. Increasing the Number of Gray Shades in Medical Display Systems—How Much is Enough? *Journal of Digital Imaging* 20, 422–432. doi:10.1007/s10278-006-1052-3.
- Kwon, J., Choi, K., 2020. Trainable Multi-contrast Windowing for Liver CT Segmentation, in: 2020 IEEE International Conference on Big Data and Smart Computing (BigComp), pp. 169–172. doi:10.1109/BigComp48618.2020.00-80.
- Lee, H., Kim, M., Do, S., 2018. Practical Window Setting Optimization for Medical Image Deep Learning. arXiv:1812.00572 [cs] arXiv:1812.00572.
- Loshchilov, I., Hutter, F., 2019. Decoupled Weight Decay Regularization. doi:10.48550/arXiv.1711.05101, arXiv:1711.05101.
- Maier, A., Steidl, S., Christlein, V., Hornegger, J. (Eds.), 2018. *Medical Imaging Systems: An Introductory Guide*. volume 11111 of *Lecture Notes in Computer Science*. Springer International Publishing, Cham. doi:10.1007/978-3-319-96520-8.

- Rajpurkar, P., Irvin, J., Zhu, K., Yang, B., Mehta, H., Duan, T., Ding, D., Bagul, A., Langlotz, C., Shpanskaya, K., 2017. Chexnet: Radiologist-level pneumonia detection on chest x-rays with deep learning. arXiv preprint arXiv:1711.05225 doi:10.48550/arXiv.1711.05225, arXiv:1711.05225.
- Wang, X., Peng, Y., Lu, L., Lu, Z., Bagheri, M., Summers, R.M., 2017. ChestX-ray8: Hospital-scale Chest X-ray Database and Benchmarks on Weakly-Supervised Classification and Localization of Common Thorax Diseases, in: 2017 IEEE Conference on Computer Vision and Pattern Recognition (CVPR), pp. 3462–3471. doi:10.1109/CVPR.2017.369, arXiv:1705.02315.
- Wollek, A., Graf, R., Čečátka, S., Fink, N., Willem, T., Sabel, B.O., Lasser, T., 2023a. Attention-based Saliency Maps Improve Interpretability of Pneumothorax Classification. Radiology: Artificial Intelligence , e220187doi:10.1148/ryai.220187.
- Wollek, A., Willem, T., Ingrisich, M., Sabel, B., Lasser, T., 2023b. A knee cannot have lung disease: Out-of-distribution detection with in-distribution voting using the medical example of chest X-ray classification. arXiv:2208.01077.
- Xiao, J., Bai, Y., Yuille, A., Zhou, Z., 2023. Delving into masked autoencoders for multi-label thorax disease classification, in: Proceedings of the IEEE/CVF Winter Conference on Applications of Computer Vision, pp. 3588–3600.